Multislice CT combined with miR-let-7 for colon cancer diagnosis and miR-let-7 targeting HMGA2 to regulate cell cycle alterations in colon cancer cells

K. Yang[1] and Z. Chen[2*]

[1]*Department of Infectious Surgery, The Affiliated Changsha Hospital of Xiangya School of Medicine, Central South University, Changsha, China*
[2]*Department of General Surgery, The Affiliated Changsha Hospital of Xiangya School of Medicine, Central South University, Changsha, China*

► *Original article*

ABSTRACT

Background: Colon cancer (CC) is one of the most common malignancies in the digestive tract. In this study, we analysed the diagnostic value of multislice CT (MSCT) in combination with miR-let-7 in CC and the mechanism of action of miR-let-7 in CC. *Materials and Methods:* A total of 108 patients with suspected CC admitted to our hospital between March 2020 and May 2022 were retrospectively analysed; 37 patients were diagnosed with CC, and the remaining 71 were determined to have benign colonic lesions. To compare the diagnostic value of MSCT, miR-let-7, and MSCT combined with miR-let-7 detection for CC, we detected the expression of miR-let-7 and high mobility group AT hook protein 2 (HMGA2) in normal human colonic epithelial FHC cells and human colonic mucosal epithelial HCT116 cells and observed the effect of miR-let-7 on the biological behaviour of CC cells. *Results:* Compared with the results of pathological biopsy, the diagnostic sensitivity of MSCT combined with miR-let-7 for CC was 97.30%, the specificity was 98.59%, and the accuracy was 98.15%, with a misdiagnosis rate of only 1.85%. After miR-let-7 expression was silenced, the viability of colon cancer cells increased, and the inflammatory response and oxidative stress increased. In addition, there was a targeted regulatory relationship between HMGA2 and miR-let-7, which could reverse the effect of miR-let-7 on colon cancer cells. *Conclusion:* The combination of MSCT and the miR-let-7 assay is accurate for the diagnosis of CC, and miR-let-7 regulates the biological behaviour of CC cells through HMGA2.

INTRODUCTION

Colon cancer (CC), a malignancy originating from the mucosal epithelium of the colon, has an extremely high incidence of 50/100,000 worldwide [1]. Notably, there has been a growing trend towards a younger age of onset of CC, with a rising prevalence in individuals under the age of 45 [2]. CC is characterized by its insidious nature, rapid progression, and poor prognosis, with 5-year mortality reaching as high as 50% [3], indicating that it poses a great potential threat. Despite some advancements in the clinical management of CC over the past few decades, overall patient survival rates have not improved as expected [4]. Therefore, a deeper understanding of the pathological mechanisms underlying CC and the exploration of new diagnostic and treatment approaches are crucial for ensuring better patient outcomes.

Multislice CT (MSCT) remains a widely utilized method for the early diagnosis of CC. MSCT is capable of producing high-resolution images that accurately identify CC primary lesions, evaluate invasion and metastasis, and offer crucial information for tumour characterization and clinical staging [5]. Despite these advantages, studies have revealed that MSCT has limited sensitivity in detecting small-diameter tumour lesions, and its subjective interpretation may lead to potential risks of leakage and misdiagnosis [6]. Consequently, there is an immediate need to identify an objective and precise clinical index that can complement MSCT, increase the early diagnosis rate of CC, and ensure increased safety for patients.

Molecular pathogenesis research has become a hot topic in cancer studies. The let-7 miRNA family plays a crucial role in the biological processes of cancer cells and is widely recognized as a tumour-suppressive miRNA; it participates in the regulation of anticancer pathways and is abnormally expressed in various tumour tissues, including CC [7, 8]. However, the exact mechanisms of action of miR-let-7 in CC are still unclear. Wang X *et al.* suggested that miR-let-7 downregulates axon guidance genes during peripheral nerve regeneration, thereby regulating the migration ability of neurogliocytes and promoting the progression of

intestinal and renal fibrosis [9]. These findings indicate the potential importance of miR-let-7 in the diagnosis and treatment of CC. In our preliminary research, we identified potential downstream target genes of miR-let-7, including high mobility group AT hook protein 2 (HMGA2), which has been extensively validated to be associated with CC [10, 11], further highlighting the potential connection between miR-let-7 and CC.

However, there are no direct studies confirming the role of miR-let-7 in CC. Therefore, the present study analysed the effect of MSCT combined with miR-let-7 on the diagnostic assessment of CC and further explored the effect of miR-let-7, which targets HMGA2, on CC to confirm the relationship between miR-let-7 and CC, thus providing valuable research references for the diagnosis and treatment of CC in the future and laying a solid foundation for subsequent studies.

MATERIALS AND METHODS

Study population

A total of 108 patients with suspected CC admitted to our hospital between March 2020 and May 2022 were retrospectively analysed. All participants underwent multislice spiral computed tomography (MSCT) and miR-let-7 testing at our facility. Following pathological biopsy, 37 patients were diagnosed with CC (research group), and the remaining 71 were determined to have benign colonic lesions (control group). This study received approval from the Ethics Committee (No. 2023-231) of the Affiliated Changsha Hospital of Xiangya School of Medicine and was carried out in strict accordance with the *Declaration of Helsinki.*

Inclusion and exclusion criteria

The inclusion criteria were as follows: (1) patients with CC and benign colonic lesions were diagnosed by pathologic examination; (2) those with complete clinical data; (3) those who did not receive related drugs or surgical treatment; and (4) all study subjects were informed and voluntarily participated in the study. The exclusion criteria were as follows: (1) those who had other malignant tumours; (2) those who had contraindications to MSCT examination or excessive image artifacts, which affected the diagnostic judgement; (3) those who had severe lesions of the heart, liver, kidney or other important organs and tissues; (4) women who were pregnant or lactating; and (5) those who were mentally and cognitively impaired and had poor obedience.

MSCT examination

The MSCT examination (GE Optima CT660, USA) was conducted upon admission of the study subjects to the hospital. Patients were directed to consume 1 bag of compound polyethylene glycol electrolyte dispersion (II) (68.56 g) per the instructions to prepare their bowels 4–6 days before the examination. The participants were placed in a supine position, and a full abdominal volume scanning mode was employed from the liver apex to the pelvic floor. The scanning parameters were set as follows: tube voltage of 120 kV, automatic tube current, layer thickness of 5 mm, and pitch of 5 mm. After the scan, 1.0–1.2 mL/kg iophedrol (Jiangsu Hengrui Pharmaceutical Co., Ltd., H20143027) was intravenously injected through the elbow at a rate of 3–5 mL/s. The arterial and portal phases were then captured, followed by arterial, portal, and delayed phase enhancement scans. The scanned images were transferred to the background processing system for assessment. Two radiologists independently reviewed the images using a double-blind method, and a consensus was reached to determine the final diagnostic outcome.

miR-let-7 expression assay

Fasting venous blood samples were drawn from the study subjects, and total ribonucleic acid (RNA) was extracted from the cells using TRIzol (Thermo Fisher, USA). The extracted RNA was then reverse transcribed into complementary deoxyribonucleic acid (cDNA) using a reverse transcription kit (Thermo Fisher, USA). The primers used were designed and constructed by GENEWIZ Suzhou, China (table 1). Two microlitres of the reverse transcription product was used as a polymerase chain reaction (PCR) amplification template, and miR-let-7 expression was determined using a fluorescence-based quantitative method under the following conditions: 95 °C for 10 s, 58 °C for 10 s, and 72 °C for 10 s. The quantitative results were analysed by the $2^{-\Delta\Delta Ct}$ method.

Table 1. Primer sequences used in the study.

	Forward sequence (5'-3')	Reverse sequence (5'-3')
miR-let-7	UUGUACUACAC AAAAGUACUG	CUAUACAACCU ACUACCUCAUU
β-actin	ATCAAGATCATT-GCTCCTCCTGAG	CTGCTT-GCTGATCCACATCTG

Determination of diagnostic efficacy

In cases of MSCT, pathologic biopsy was used as the gold standard to calculate the diagnostic yield. For miR-let-7, receiver operating characteristic (ROC) curves were generated to assess miR-let-7 expression in both the study and control groups, and the optimal sensitivity and specificity at specific cut-off values were determined. In the combined test, miR-let-7 was qualitatively evaluated using the designated cut-off value, where cases presenting positive results for both MSCT and miR-let-7 were considered positive for the combined test and compared to the results of pathological biopsies.

Cell information

Normal human colonic epithelial cells (FHC) and human colonic mucosal epithelial cells (HCT116)

were obtained from BeNa Culture Collection (China). The cells were placed in Dulbecco's modified Eagle's medium (DMEM) for adherent culture in a humidified incubator maintained at 37 °C with 5% CO_2, followed by cell passage.

miR-let-7 expression determination

FHC and HCT116 cells were inoculated into 6-well plates (Thermo Fisher, USA) at 2×10^5 cells/well, followed by detection of miR-let-7 expression as described above.

Determination of HMGA2 expression

The total proteins of FHC and HCT116 cells were separated for concentration determination using the standard curve method, followed by sodium dodecyl sulphate–polyacrylamide gel electrophoresis (SDS–PAGE) (Thermo Fisher, USA), membrane transfer, blocking with 5% skim milk at room temperature for l h, and the addition of primary antibodies (HMGA2 1:200, GAPDH 1:2000) (Abcam, UK) for incubation at 4 °C overnight. The mixture was subsequently washed with Tris-buffered saline 3 times (10 min each), incubated with secondary antibody (1:1000) (Abcam, UK) for 2 h at ambient temperature, and washed 3 times (10 min each). Finally, exposure treatment was performed following the instructions for enhanced chemiluminescence (ECL) (Shanghai Yanxi Biotechnology Co., Ltd., China), and grayscale analysis was performed with QuantityOne software (Bio-Rad, USA).

Effect of miR-let-7 on HMGA2

The cells were collected, adjusted to 1×10^5/well, and inoculated into 6-well plates. Two millilitres of cell suspension was added to each well and cultured at 37 °C with 5% CO_2 for 24 h and then divided into three groups: the miR-let-7 mimic-transfected group (miR-let-7-mim group), the miR-let-7 inhibitor-transfected group (miR-let-7-inh group), and the miR-let-7 negative control-transfected group (miR-let-7-nc group). Transfection was performed following the instructions for Lipofectamine 2000.

Validation of targeted relationships

The downstream target genes of miR-let-7 and the complementary binding sites with HMGA2 were identified using the online target gene prediction website TargetScan. Wild-type (WT) and mutant (MUT) HMGA2 were separately cloned and inserted into pMIR-REPORT luciferase reporter vectors. HCT116 cells were inoculated in 24-well plates at 6×10^5 cells/well and incubated for 24 h. miR-let-7-mim and miR-let-7-nc were cotransfected into HCT116 cells using Lipofectamine 2000 (Thermo Fisher, USA), and the luciferase activity was measured by dual-luciferase assay (MCE, USA) 48 h later.

Cell viability assay

The miR-let-7-mim, miR-let-7-inh, and miR-let-7-nc groups were established according to the aforementioned methods, as was an additional group cotransfected with the miR-let-7-inh plus silenced HMGA2 expression vector (miR-let-7-inh+HMGA2-inh group). At 24, 48, 72, and 96 h after transfection, 5 mg/mL MTT (Shanghai Enzyme Link Technology Co., Ltd., China) was added to each well, and after supernatant removal, 200 µL of dimethyl sulfoxide was added. The absorbance value (490 nm) was measured. Additionally, 200 cells from each group were inoculated in 6-well plates, fixed with 4% paraformaldehyde, and stained with crystal violet. The cell cloning efficiency was calculated as follows:

Cell cycle analysis

The cells from each group were incubated in cold 70% ethanol overnight, washed with PBS, and stained with a cell cycle analysis kit in the dark for 30 min. The cell cycle distribution was analysed by flow cytometry (Attune NxT, Thermo Fisher, USA).

Inflammatory response and stress monitoring

The cell culture suspensions from each group were centrifuged, and the supernatants were obtained for the measurement of tumour necrosis factor-α (TNF-α), interleukin-1β (IL-1β), interleukin-6 (IL-6), superoxide dismutase (SOD), malondialdehyde (MDA), and glutathione peroxidase (GSH-Px) levels following the instructions of the enzyme-linked immunosorbent assay kit (Shanghai Sunlight Biotechnology Co., Ltd., China).

Statistical analysis

Statistical analysis was performed using SPSS 22.0 (IBM, USA), and all the results are expressed as (`c±s). The diagnostic compliance rate was analysed using the kappa test, and the diagnostic value of miR-let-7 was analysed using the ROC curve. Independent sample t tests were used for comparisons between two groups, and repeated measures analysis of variance (ANOVA) and the Bonferroni post hoc correction were used for comparisons across multiple time points. Statistical significance was defined as $P<0.05$.

RESULTS

Diagnostic results of MSCT for CC

Figure 1 shows common CC imaging features, including the presence of a visible mass shadow within the intestinal lumen, abnormal thickening of the colonic wall, and potential increased density shadows in the surrounding fat layer around the colonic lesion. Moreover, CT scans in certain patients may reveal signs of intestinal obstruction, characterized by the presence of fluid and gas in the intestinal lumen and dilation of the intestinal tract. In cases of CC perforation, a gas collection shadow may be observed in the lesion area. After MSCT

examination, 40 out of the 108 study subjects were diagnosed with CC. Compared with the pathological biopsy results, the diagnostic sensitivity, specificity, accuracy and misdiagnosis rate of MSCT for CC were 89.19%, 90.14%, 89.81% and 10.19% (Kappa=0.859), respectively, which were high reference values (table 2).

Table 2. Diagnostic efficacy of MSCT for CC.

		Pathological biopsy			Sensitivity	Specificity	Accuracy	False diagnosis rate
		(+)	(-)	Total				
MSCT	(+)	33	7	40	89.19	90.14	89.81	10.19
	(-)	4	64	68				
	Total	37	71					

Diagnostic effect of miR-let-7 on CC

The results revealed that the levels of miR-let-7 were 1.47±0.54 in the research group and 2.25±0.67 in the control group. A comparison of the two groups revealed that the level of miR-let-7 in the research group was even lower than that in the control group (P<0.05). The ROC curve revealed that the sensitivity and specificity for diagnosing the occurrence of CC were 91.89% and 63.38%, respectively, when the miR-let-7 level was <2.04 (P<0.05) (figure 2).
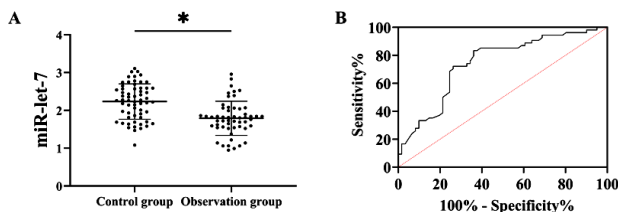

Figure 2. Diagnostic effect of miR-let-7 on CC. **(A)** Comparison of miR-let-7 expression between the research and control groups. **(B)** ROC curve of miR-let-7 for the diagnosis of CC occurrence.

Diagnostic effect of MSCT combined with miR-let-7 on CC

MSCT combined with miR-let-7 revealed that 37 of the 108 study subjects were diagnosed with CC. Compared with the results of pathological biopsy, the diagnostic sensitivity of MSCT combined with miR-let-7 for CC was 97.30%, the specificity was 98.59%, and the accuracy was 98.15%, with a misdiagnosis rate of only 1.85% (Kappa=0.956), which had a high reference value (table 3).

Table 3. Diagnostic effect of MSCT combined with miR-let-7 on CC.

		Pathological biopsy			Sensitivity	Specificity	Accuracy	False diagnosis rate
		(+)	(-)	Total	97.30	98.59	98.15	1.85
MSCT +miR-let-7	(+)	36	1	37				
	(-)	1	70	71				
	Total	37	71					

Expression of miR-let-7 and HMGA2 in CC

The results of the qPCR and western blot analyses revealed that, compared with those in FHC cells, miR-let-7 expression was significantly lower and HMGA2 protein expression was significantly elevated

in HCT116 CC cells (P<0.05). These results suggest that miR-let-7 is downregulated and that HMGA2 is upregulated in CC (figure 3).
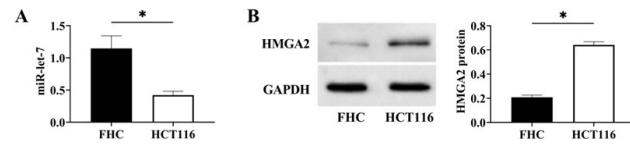

Figure 3. Expression of miR-let-7 and HMGA2 in CC. **A)** Expression levels of miR-let-7 in FHC and HCT116 cells. **B)** Expression levels of the HMGA2 protein in FHC and HCT116 cells. *P<0.05. High mobility group AT hook protein 2, HMGA2; normal human colonic epithelial cells, FHC; and human colonic mucosal epithelial cells, HCT116.

Relationship between miR-let-7 and HMGA2

The expression of miR-let-7 in the miR-let-7-mim group was greater than that in the miR-let-7-nc group, whereas the expression of miR-let-7 in the miR-let-7-inh group was lower than that in the miR-let-7-nc group (P<0.05). HMGA2 expression was lower in the miR-let-7-mim group than in the miR-let-7-nc group, whereas the expression of HMGA2 in the miR-let-7-inh group was greater than that in the miR-let-7-nc group (P<0.05). The online database revealed complementary binding sites between miR-let-7 and HMGA2, as illustrated in Figure 2C. The luciferase assay results revealed that the fluorescence activity of HMGA2-WT was notably inhibited after transfection with miR-let-7-mim (P<0.05), confirming the targeting relationship between the two groups (figure 4).
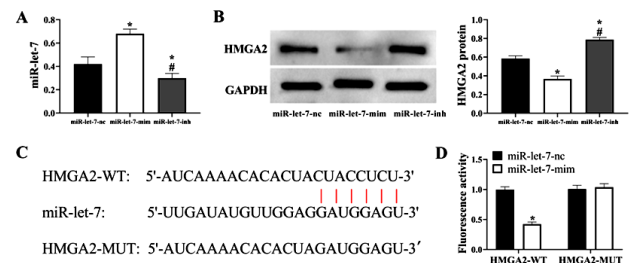

Figure 4. Relationship between miR-let-7 and HMGA2. **A)** Detection of miR-let-7 expression to verify the success rate of transfection. **B)** Effect of miR-let-7 on HMGA2 protein expression. **C)** Bindable complementary sites of miR-let-7 and HMGA2. **D)** Luciferase activity assay. vs. the miR-let-7-nc group, *P<0.05; vs. the miR-let-7-mim group, #P<0.05. Wild-type, WT; Mutant-type, MUT.

Effect of miR-let-7 targeting HMGA2 on CC cell viability

According to the results of the cell biology assays, compared with that in the miR-let-7-nc group, the growth ability of the cells in the miR-let-7-mim group was lower, that in the miR-let-7-inh group was greater, and that in the miR-let-7-inh+HMGA2-inh group was comparable. The cell cloning efficiencies in the miR-let-7-nc, miR-let-7-mim, miR-let-7-inh, and miR-let-7-inh+HMGA2-inh groups were 56.52±3.18%, 28.34±1.71%, 81.90±2.40%, and 54.99±1.52%, respectively. There was no difference between the

miR-let-7-nc group and the miR-let-7-inh+ HMGA2-inh group in terms of cloning efficiency (P>0.05); the efficiency was highest in the miR-let-7-inh group and lowest in the miR-let-7-mim group (P<0.05). In the cell cycle analysis, no marked difference was observed between the miR-let-7-nc group and the miR-let-7-inhibitor+HMGA2-inhibitor group (P>0.05). However, the G0/G1 phase was shortened in the miR-let-7-mim group, whereas the G0/G1 phase was prolonged in the miR-let-7-inh group compared with the other three groups (P<0.05) (figure 5).

Effects of miR-let-7 targeting HMGA2 on the inflammatory response and oxidative stress in CC cells

The results of the inflammatory response and

oxidative stress assays revealed no statistically significant differences in any indicators between the miR-let-7-nc and miR-let-7-inh+HMGA2-inh groups (P>0.05). The expression levels of IL-1β, IL-6, TNF-α, and MDA in the miR-let-7-mim group were lower than those in the miR-let-7-nc and miR-let-7-inh+HMGA2-inh groups, whereas the SOD and GSH-Px levels were greater (P<0.05); the expression levels of IL-1β, IL-6, and TNF-α in the miR-let-7-inh group and the MDA level were greater than those in the miR-let-7-nc and miR-let-7-inh+HMGA2-inh groups, whereas the SOD and GSH-Px levels were lower (P<0.05) (Figure 6).
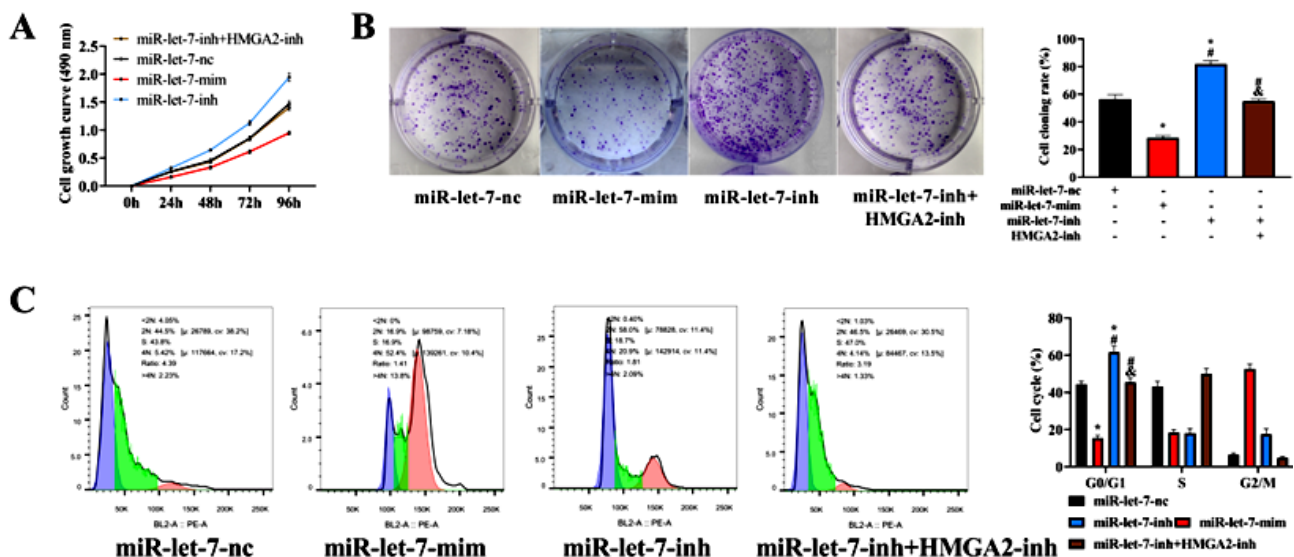

Figure 5. Effect of miR-let-7 targeting HMGA2 on CC cell viability. A) Cell growth curves. B) Cell clonogenicity. C) Cell cycle alterations. vs. the miR-let-7-nc group, *P<0.05; vs. the miR-let-7-mim group #P<0.05; vs. the miR-let-7-inh group, &P<0.05.

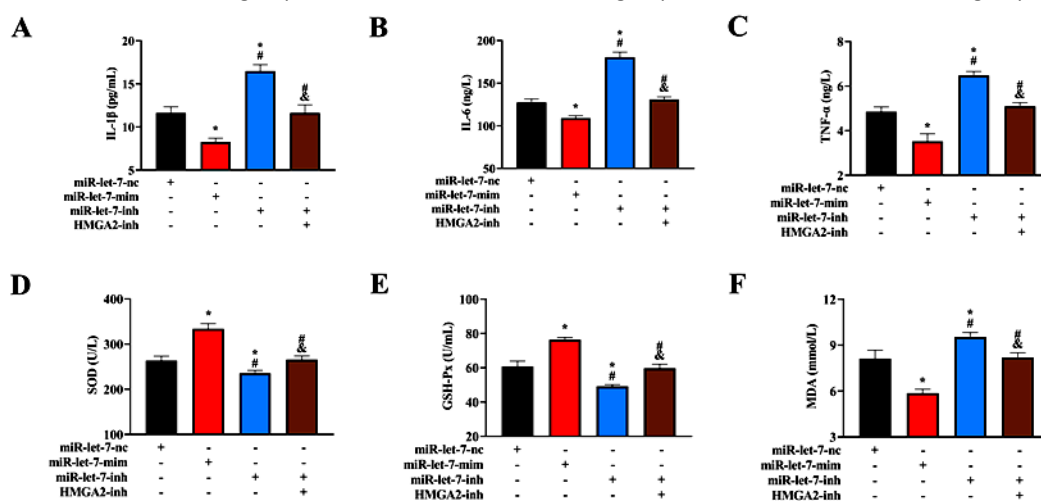**Figure 6.** Effects of miR-let-7 targeting HMGA2 on the inflammatory response and oxidative stress in CC cells. **A)** Comparison of IL-1β levels. **B)** Comparison of IL-6 levels. **C)** Comparison of TNF-α levels. **D)** Comparison of SOD levels. **E)** Comparison of GSH-Px levels. **F)** Comparison of MDA levels. vs. the miR-let-7-nc group, *P<0.05; vs. the miR-let-7-mim group, #P<0.05; vs. the miR-let-7-inh group, &P<0.05. tumour necrosis factor-α, TNF-α; interleukin-1β, IL-1β; interleukin-6, IL-6; superoxide dismutase, SOD; malondialdehyde, MDA; glutathione peroxidase, GSH-Px.

DISCUSSION

Over the years, the incidence of CC has shown an increasing trend and a shift towards younger age groups, posing a significant potential threat to patient prognosis and survival [12]. In this study, we analysed the effect of MSCT combined with miR-let-7 on the diagnostic assessment of CC, which can provide new references and guidelines for the future clinical diagnosis of CC.

First, we examined the diagnostic potential of MSCT and miR-let-7 for CC. The findings revealed that the typical MSCT image characteristics of CC included a mass in the intestinal lumen, abnormal thickening of the colon wall, and increased density of the fat layer surrounding the colon lesion, which are consistent with the clinical imaging guidelines for CC [13]. Subsequent analysis compared the visible and pathological biopsy results, with MSCT demonstrating a diagnostic sensitivity, specificity, and accuracy for CC of 89.19%, 90.14%, and 89.81%, respectively. In a cross-sectional study by Li Q et al., where MSCT images of 100 subjects were analysed, the diagnostic sensitivity and specificity for CC were 83.11% and 84.99%, respectively, which aligns closely with our results [14]. Previous research has emphasized the significant role of MSCT in the qualitative diagnosis of malignant tumours; its increasing utilization, particularly CT postprocessing technology, offers comprehensive insight into lesion characteristics from various perspectives [15]. Despite the benefits, depending solely on MSCT may not capture the full organ structure and subtle lesion changes [16], as evidenced by the six misdiagnosed and omitted patients in our study.

As a genetic product in the human body, miR-let-7 can be detected in a variety of samples, such as blood, body fluids, tissues, and cells; thus, it has gradually become a hotspot in the clinical diagnostic research of various tumour diseases in recent years. miR-let-7, a hotspot in modern molecular oncology research, has been found to have important impacts on the growth processes of various tumours (e.g., tongue cancer and melanoma) [17, 18]. However, its relationship with CC remains unclear. In this study, we initially assessed the expression of miR-let-7 in colorectal cancer (CC), revealing significantly lower levels in the research group than in the control group. These findings suggest an abnormal downregulation of miR-let-7 in CC, potentially indicating its role in the onset and progression of this disease. Subsequent ROC curve analysis revealed that the diagnostic sensitivity and specificity of miR-let-7 for CC were 91.89% and 63.38%, respectively, with an AUC of 0.813, indicating considerable diagnostic utility. Combining MSCT and miR-let-7 detection yielded a protocol with a diagnostic sensitivity, specificity, and accuracy for CC of 97.30%, 98.59%, and 98.15%, respectively, and a kappa value of 0.956, aligning

closely with pathological biopsy outcomes and demonstrating high diagnostic potential. The inclusion of miR-let-7 may compensate for the limitations of MSCT in detecting minute lesions. Furthermore, objective quantitative analysis results can validate MSCT findings, enhancing diagnostic performance. The integration of MSCT with miR-let-7 detection in clinical settings holds promise for enhancing the early detection rate of CC, thereby improving patient prognosis.

To further validate the expression of miR-let-7 in CC, we subsequently measured miR-let-7 in FHC and HCT116 cells. The level of miR-let-7 was significantly lower in HCT116 cells than in FHC cells, indicating that miR-let-7 was expressed at low levels in CC, which is consistent with the findings of similar studies [19]. To further confirm the effect of miR-let-7 on CC, we subsequently investigated the expression of miR-let-7 with aberrant expression sequences. miR-let-7 expression silencing resulted in increased activity in HCT116 cells and a prolonged G0/G1 phase, suggesting that low expression of miR-let-7 plays an oncogenic role in CC, accelerating its malignant progression. Conversely, elevated miR-let-7 markedly inhibited the proliferative capacity of HCT116 cells and shortened the G0/G1 phase, suggesting that upregulated miR-let-7 promotes CC cell apoptosis. Furthermore, the cell inflammatory response and oxidative stress were significantly intensified following miR-let-7 expression silencing, demonstrating that downregulated miR-let-7 contributes to cellular damage in CC, accelerating its malignant progression. The pathological progression described above could be improved when miR-let-7 was elevated. Taken together, these results suggest that targeted molecular therapy to increase miR-let-7 levels holds promise as a novel treatment approach for CC. Indeed, the effects of miR-let-7 on ovarian cancer and pulmonary fibrosis, such as the promotion of ovarian cancer cell growth, migration, and invasion by the lncRNA NEAT1 through miR-let-7 [20] and the improvement of pulmonary fibrosis by ferroptosis inhibition through the Sp3/HDAC2/Nrf2 signalling pathway via miR-let-7 in the exosomes of vesicle-derived stem cells [21], have been established. These findings indicate that extensive experimentation and research are still needed to validate the clinical application of targeted molecular therapy utilizing miR-let-7 for CC.

In addition, miR-let-7 is associated with endothelial cell injury [22] and enhances uterine receptivity by inhibiting the Wnt/β-catenin pathway [23]. However, its specific mechanisms of action in CC are still unclear. In the prediction and analysis of downstream target genes, HMGA2 has attracted our attention. The HMGA2 rs968697 T>C polymorphism is associated with the risk of CC [24], and HMGA2 promotes malignant behaviour in CC through the transcriptional activation of FN1 and IL11 [25]. These

studies established a potential link between HMGA2 and CC. In the present study, we also found that HMGA2 protein expression was greater in HCT116 cells than in FHC cells, which is consistent with the above findings. The fluorescence activity of HMGA2-WT was inhibited by miR-let-7, confirming the targeting relationship [26]. MiR-let-7 elevation led to decreased HMGA2 in HCT116 cells, whereas miR-let-7 silencing achieved the opposite results. Taken together, these results suggest that miR-let-7 participates in CC progression by increasing HMGA2 in a targeted manner. After cotransfection with miR-let-7-inh and HMGA2-inh, the biological behaviours, inflammatory responses, and oxidative stress responses in this group were consistent with those in the miR-let-7-nc group, suggesting that the effects of miR-let-7 silencing on CC cells were completely reversed after HMGA2 silencing, which verified the targeted regulatory relationship between the two. These findings will help us gain a deeper understanding of the specific mechanisms by which miR-let-7 is involved in CC.

However, clinical cases were not included in this study for confirmation; therefore, the clinical significance of miR-let-7 in CC cannot be evaluated herein. Additionally, more in-depth experiments are needed to further confirm the mechanisms and pathways through which miR-let-7 affects CC. In the future, more in-depth and comprehensive analyses will be conducted to address these limitations and provide more reliable references for clinical practice.

In summary, the combination of MSCT and the miR-let-7 assay is accurate for the diagnosis of CC and can be used as an early screening protocol for CC for clinical reference. In addition, miR-let-7 was downregulated in CC and promoted malignant proliferation, the inflammatory response, and oxidative stress by targeting HMGA2, accelerating CC progression. In the future, molecular therapy targeting the upregulation of miR-let-7 may become a new therapeutic direction for CC.

Data availability: Original data in this study are available from the corresponding author on reasonable requests.

Conflicts of interest statement: None declared.

Ethical considerations: This study received approval from the Ethics Committee (No. 2023-231) of the Affiliated Changsha Hospital of Xiangya School of Medicine and was carried out in strict accordance with the *Declaration of Helsinki*.

Author contributions: KY: performed the experiments, collected the data, and drafted the manuscript, responsible for data analysis and visualization; ZC: conceived and designed the study, and was a major contributor in critically revising the manuscript. All authors read and approved the final manuscript.

REFERENCES

1. Fabregas JC, Ramnaraign B, George TJ (2022) Clinical updates for colon cancer care in 2022. *Clinical Colorectal Cancer, 21(3): 198-203.*
2. Smart N (2023) Colon cancer care is changing and not before time. *Colorectal Disease, 25(3): 351.*
3. Jahanafrooz Z, Mosafer J, Akbari M, *et al.* (2020) Colon cancer therapy by focusing on colon cancer stem cells and their tumor microenvironment. *Journal of Cellular Physiology, 235(5): 4153-4166.*
4. Yalcin S, Philip PA, Athanasiadis I, *et al.* (2022) Classification of early-stage colon cancer with Immunoscore ((R)): clinical evidence and case studies. *Future Oncology, 18(5): 613-623.*
5. Fernandez LM, Parlade AJ, Wasser EJ, *et al.* (2019) How reliable is CT scan in staging right colon cancer? *Diseases of the Colon & Rectum, 62(8): 960-964.*
6. Wetterholm E, Rosen R, Rahman M, *et al.* (2023) CT is unreliable in locoregional staging of early colon cancer: A nationwide registry-based study. *Scandinavian Journal of Surgery, 112(1): 33-40.*
7. Su JL, Chen PS, Johansson G, *et al.* (2012) Function and regulation of let-7 family microRNAs. *Microrna, 1(1): 34-39.*
8. You X, Liu M, Liu Q, *et al.* (2022) miRNA let-7 family regulated by NEAT1 and ARID3A/NF-kappaB inhibits PRRSV-2 replication in vitro and in vivo. *PLoS Pathog, 18(10): e1010820.*
9. Wang X, Chen Q, Yi S, *et al.* (2019) The microRNAs let-7 and miR-9 down-regulate the axon-guidance genes Ntn1 and Dcc during peripheral nerve regeneration. *Journal of Biological Chemistry, 294 (10): 3489-3500.*
10. Liu HH, Lee CH, Hsieh YC, *et al.* (2021) Multiple myeloma driving factor WHSC1 is a transcription target of oncogene HMGA2 that facilitates colon cancer proliferation and metastasis. *Biochem Biophys Res Comm, 567: 183-189.*
11. Chen CH, Hsieh YC, Yang PM, *et al.* (2020) Dicoumarol suppresses HMGA2-mediated oncogenic capacities and inhibits cell proliferation by inducing apoptosis in colon cancer. *Biochem Biophys Res Comm, 524(4): 1003-1009.*
12. Taieb J, Karoui M, Basile D (2021) How I treat stage II colon cancer patients. *ESMO Open, 6(4): 100184.*
13. Obaro AE, Burling DN, Plumb AA (2018) Colon cancer screening with CT colonography: logistics, cost-effectiveness, efficiency and progress. *British Journal of Radiology, 91(1090): 20180307.*
14. Li Q, Dai P, Zhang W, *et al.* (2024) Improved diagnostic accuracy of multi-slice spiral CT combined with MRI in colon cancer patients with ileus: A comparative study. *Alternative Therapies in Health and Medicine, Published online March 8, 2024.*
15. Hong EK, Castagnoli F, Gennaro N, *et al.* (2021) Locoregional CT staging of colon cancer: does a learning curve exist? *Abdominal Radiology (NY), 46(2): 476-485.*
16. Hong EK, Landolfi F, Castagnoli F, *et al.* (2021) CT for lymph node staging of Colon cancer: not only size but also location and number of lymph node count. *Abdominal Radiology (NY), 46(9): 4096-4105.*
17. Kou N, Liu S, Li X, *et al.* (2019) H19 facilitates tongue squamous cell carcinoma migration and invasion via sponging miR-let-7. *Oncology Research, 27(2): 173-182.*
18. Liu YX, Bai JX, Li T, *et al.* (2019) MiR-let-7a/f-CCR7 signalling is involved in the anti-metastatic effects of an herbal formula comprising Sophorae Flos and Lonicerae Japonicae Flos in melanoma. *Phytomedicine, 64: 153084.*
19. Joshi S, Wei J, Bishopric NH (2016) A cardiac myocyte-restricted Lin28/let-7 regulatory axis promotes hypoxia-mediated apoptosis by inducing the AKT signalling suppressor PIK3IP1. *Biochimica et Biophysica Acta, 1862(2): 240-251.*
20. Yin L, Wang Y (2021) Long non-coding RNA NEAT1 facilitates the growth, migration, and invasion of ovarian cancer cells via the let-7 g/MEST/ATGL axis. *Cancer Cell International, 21(1): 437.*
21. Sun L, He X, Kong J, *et al.* (2024) Menstrual blood-derived stem cells exosomal miR-let-7 to ameliorate pulmonary fibrosis through inhibiting ferroptosis by Sp3/HDAC2/Nrf2 signalling pathway. *International Immunopharmacology, 126: 111316.*
22. Cao L, Zhang Z, Li Y, *et al.* (2019) LncRNA H19/miR-let-7 axis partici-

pates in the regulation of ox-LDL-induced endothelial cell injury via targeting periostin. *International Immunopharmacology, 72: 496-503.*

23. Li Q, Liu W, Chiu PCN, *et al.* (2020) Mir-let-7a/g enhances uterine receptivity via suppressing Wnt/beta-catenin under the modulation of ovarian hormones. *Reproductive Sciences, 27 (5): 1164-1174.*

24. Gao X and Wang X (2021) HMGA2 rs968697 T > C polymorphism is associated with the risk of colorectal cancer. *Nucleosides Nucleotides Nucleic Acids, 40(8): 821-828.*

25. Wu J, Wang Y, Xu X, *et al.* (2016) Transcriptional activation of FN1 and IL11 by HMGA2 promotes the malignant behaviour of colorectal cancer. *Carcinogenesis, 37(5): 511-521.*

26. Xu YZ, Kanagaratham C, Jancik S, *et al.* (2013) Promoter deletion analysis using a dual-luciferase reporter system. *Methods in Molecular Biology, 977: 79-93.*